Global CO_2 rise leads to reduced maximum stomatal conductance in Florida vegetation

Emmy I. Lammertsma[a,1], Hugo Jan de Boer[b], Stefan C. Dekker[b], David L. Dilcher[c,1], André F. Lotter[a], and Friederike Wagner-Cremer[a]

[a]Palaeoecology, Laboratory of Palaeobotany and Palynology, Institute of Environmental Biology, Utrecht University, 3584 CD, Utrecht, The Netherlands; [b]Department of Environmental Sciences, Copernicus Institute, Utrecht University, 3508 TC, Utrecht, The Netherlands; and [c]Department of Biology, Indiana University, Bloomington, IN 47405

A principle response of C3 plants to increasing concentrations of atmospheric CO_2 (CO_2) is to reduce transpirational water loss by decreasing stomatal conductance (g_s) and simultaneously increase assimilation rates. Via this adaptation, vegetation has the ability to alter hydrology and climate. Therefore, it is important to determine the adaptation of vegetation to the expected anthropogenic rise in CO_2. Short-term stomatal opening–closing responses of vegetation to increasing CO_2 are described by free-air carbon enrichments growth experiments, and evolutionary adaptations are known from the geological record. However, to date the effects of decadal to centennial CO_2 perturbations on stomatal conductance are still largely unknown. Here we reconstruct a 34% ($\pm$12%) reduction in maximum stomatal conductance (g_{smax}) per 100 ppm CO_2 increase as a result of the adaptation in stomatal density (D) and pore size at maximal stomatal opening (a_{max}) of nine common species from Florida over the past 150 y. The species-specific g_{smax} values are determined by different evolutionary development, whereby the angiosperms sampled generally have numerous small stomata and high g_{smax}, and the conifers and fern have few large stomata and lower g_{smax}. Although angiosperms and conifers use different D and a_{max} adaptation strategies, our data show a coherent response in g_{smax} to CO_2 rise of the past century. Understanding these adaptations of C3 plants to rising CO_2 after decadal to centennial environmental changes is essential for quantification of plant physiological forcing at timescales relevant for global warming, and they are likely to continue until the limits of their phenotypic plasticity are reached.

cuticular analysis | subtropical vegetation

Land plants play a crucial role in regulating our planet's hydrological and energy balance by transpiring water through the stomatal pores on their leaf surfaces. A fundamental response of C3 plants to increasing atmospheric CO_2 concentration (CO_2) is to minimize transpirational water loss by reducing diffusive stomatal conductance (g_s) and simultaneously increasing assimilation rates (1). The resulting increased intrinsic water-use efficiency (iWUE: the ratio of assimilation to g_s) improves the vegetation's drought resistance and reduces the cost associated with the leaf's water transport system like leaf venation (2, 3). On a regional to global scale, decreasing rates of transpiration concurrently affect climate through reduced cloud formation and precipitation (4) and with this exert a physiological feedback on climate and hydrology on top of the radiative forcing of increasing CO_2 (5–7). In the light of continuing anthropogenic climate change, it is therefore imperative to determine how plants adapt to rising atmospheric CO_2.

During their 400 million year history, land plants have been exposed to large variations in environmental conditions that prompted genetic adaptations toward mechanisms that optimize individual fitness. Over this period, plant adaptation to CO_2 is apparent as periods with high CO_2 favored species with few relatively large stomata and low g_s, whereas periods with low CO_2 (as at present) favored species with many relatively small sto-

mata and higher g_s (8). Moreover, decreasing CO_2 after $\approx$100 million years likely triggered the evolutionary development of a more extensive leaf vein network in angiosperms, giving them the advantage of potentially higher g_s than gymnosperms with low vein density (9). At shorter timescales, plants have the ability to adjust their phenotype to optimize gas exchange. In response to short (seconds to hours) perturbations in CO_2, plants open and close their stomata (10, 11), whereas in response to CO_2 changes at decadal to centennial timescales, plants adjust leaf stomatal density (D) and/or maximum stomatal dimensions (a_{max}) (12–15). This process of epidermal structural adaptation is in part controlled by a signaling mechanism from mature to developing leaves, optimizing stomatal density and size to the changed environmental conditions (16). These epidermal characteristics determine the anatomical maximum stomatal conductance to water vapor (g_{smax}, mol·m^{-2}·s^{-1}) of fully opened stomata and can be calculated as (8, 17):

$$g_{smax} = \frac{\frac{d_w}{v} \cdot D \cdot a_{max}}{l + \frac{\pi}{2}\sqrt{a_{max}/\pi}} \quad [1]$$

in which stomatal density [D (number of stomata·m^{-2})], the size of the fully opened stomata a_{max} (m^2), and depth of the stomatal tube l (m) are the determining variables. The diffusivity of water vapor d_w (m^2·s^{-1}) and the molar volume of air v (m^3·mol^{-1}) are constants. Values of a_{max} and l are derived from the stomatal pore length L (m). Maximum stomatal conductance to CO_2 is g_{smax}/1.6 (18).

The most comprehensive analyses of plant adaptation to elevated CO_2 in (semi)natural environments are available from free-air carbon enrichments (FACE) growth experiments (19). Although decreases in D of C3 plants did occur in some studies (20), the observed reduction in g_s was found to be caused by instantaneous adaptation only (21). Apparently, the run-time of these growth experiments of <5 y might be too short to trigger statistically significant epidermal structural adaptation (22). Consequently, the subtle adaptation of vegetation to continuously increasing CO_2 can only be elucidated from material covering periods long enough to deduce quantifiable structural adaptation. Because CO_2 has already increased by $\approx$100 ppm over the past 150 y, historical leaves preserved in sediments and stored in herbarium collections offer an excellent opportunity to study the adaptation of g_{smax} to the gradual rise in CO_2.

Because the leaf epidermal properties D and a_{max} are also influenced by other environmental factors such as light, temperature, and water availability (23–25), it is necessary to use leaf material from plants that grew under conditions in which the global CO_2 rise is the dominant variable factor. This prerequisite is met in Florida, where the vegetation has been exposed to the global $\approx$100 ppm CO_2 increase under near constant average growth season temperatures and precipitation rates over the past 150 y (Fig. 1). Moreover, structural adaptation to increasing CO_2 by decreasing D has already been demonstrated for a number of Florida forest taxa (28, 29).

Here we present a high-resolution historical record of nine C3 species that adapted g_{smax} to the 100 ppm rise in CO_2 since approximately 1880 A.D. Species studied are the woody angiosperms *Acer rubrum* (Aceraceae), *Myrica cerifera* (Myricaceae), *Ilex cassine* (Aquifoliaceae), *Quercus laurifolia* (Fagaceae), and *Quercus nigra* (Fagaceae), the conifers *Pinus elliottii* (Pinaceae), *Pinus taeda* (Pinaceae), and *Taxodium distichum* (Cupressaceae), and the fern *Osmunda regalis* (Osmundaceae). This selection embraces species with deciduous and evergreen leaf types, growing in wet to well-drained sites in upper to lower canopy layers (Table S1). The cuticle material analyzed originates from subfossil leaf fragments retrieved from well-dated young peat deposits (26, 30) as well as herbarium and modern material collected from various sites in Florida (Fig. 1).

In the present study we aim to quantify how these species have adapted g_{smax} in response to the industrial rise in CO_2. Moreover, the present selection includes multiple angiosperm and co-niferous species, of which the leaves are characterized by a high and low leaf vein density, respectively. Because angiosperms have invested more in an elaborate leaf hydraulic system (31), we raise the hypothesis that they will benefit more by reducing g_{smax} stronger to rising CO_2. The data we present here allow for quantification of plant physiological adaptation at timescales relevant for anthropogenic climate change and provide much-needed data for parameterization and validation of climate models that include these physiological feedbacks.

Results

A consistent decrease in g_{smax} over the anthropogenic rise in CO_2 is observed in all species studied ($P < 0.05$) (Fig. 2). The inferred g_{smax} values of these nine species range between $\approx$0.4 (mol·m^{-2}·s^{-1}) to $\approx$4 (mol·m^{-2}·s^{-1}), with the highest values for the angiosperm canopy species *Q. nigra*, *Q. laurifolia*, and *A. rubrum* and the lowest values for the fern *O. regalis*. Despite the large differences in absolute values of g_{smax} between species, relative sensitivities in g_{smax} over $\approx$100 ppm CO_2 rise are highly comparable, with a mean slope of −34% (±12%) per 100 ppm (Table 1). The weakest responses occur in *P. elliottii* and *Q. laurifolia*,
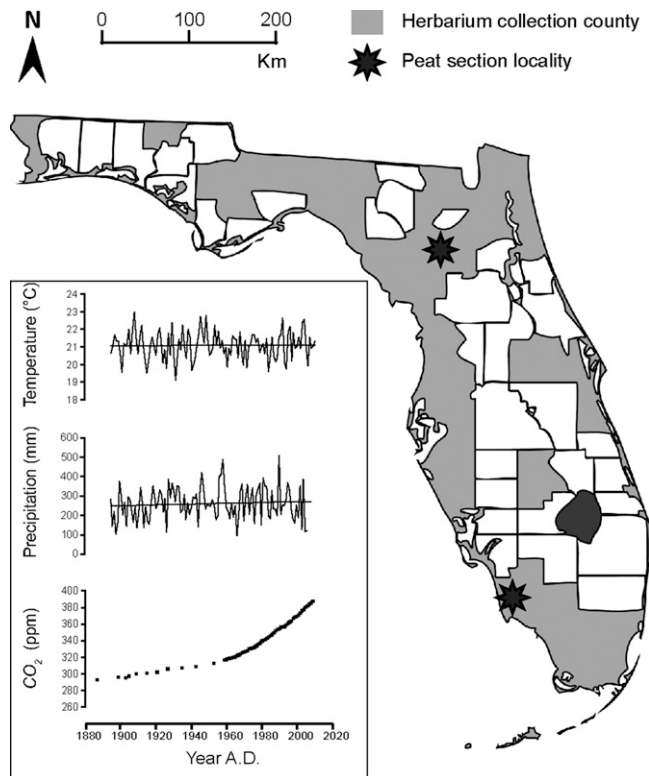
Fig. 1. Locations of leaf material collection sites in Florida: state counties covered by herbarium material (gray) and subfossil leaf fragment sites (black stars). Florida averaged spring (March, April, and May) temperature and cumulative precipitation (http://www.ncdc.noaa.gov) and global atmospheric CO_2 concentration [Siple station (26); Mauna Loa (27)] from 1880 A.D. to present are given. The various sites are situated approximately at sea level. Black lines in the temperature and precipitation graphs are long-term means of $\approx$21 °C and $\approx$260 mm, respectively.
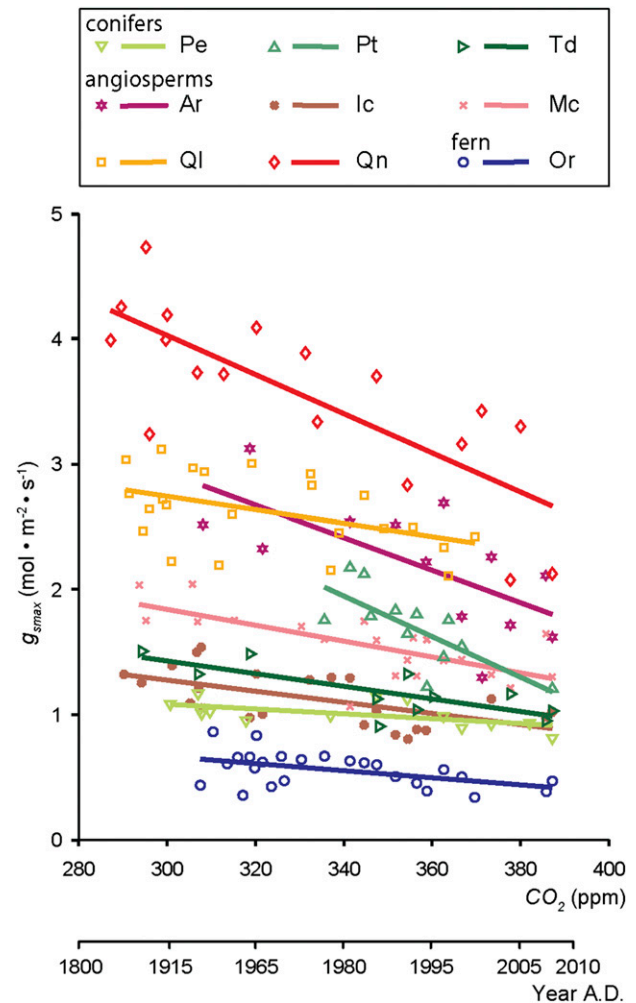
Fig. 2. Species-specific relation between g_{smax} and CO_2 over the past 150 y. Symbols are average g_{smax} (mol·m^{-2}·s^{-1}) for each species per CO_2 level (ppm) studied ($n = 160$), and accompanying year A.D. (species names and abbreviations are given in Table 1). Solid lines show linear regressions between CO_2 and g_{smax} for each species, r^2 and relative sensitivity are given in Table 1. The functions and RMSE for each species are provided in Table S2.

Lammertsma et al.

Table 1. Relative sensitivity of g_{smax}, D, and a_{max} to CO_2 increase for the species sampled (intercept, 100% at 280 ppm CO_2), with r^2 of the linear regressions used

Species	Species code	Average g_{smax}		Average stomatal density D		Average pore size a_{max}	
		Relative sensitivity (%·ppm^{-1})	r^2	Relative sensitivity (%·ppm^{-1})	r^2	Relative sensitivity (%·ppm^{-1})	r^2
Acer rubrum	Ar	−0.41*	0.45	−0.29*	0.30	−0.27*	0.40
Ilex cassine	Ic	−0.30*	0.36	−0.26*	0.38	−0.13	0.04
Myrica cerifera	Mc	−0.36*	0.49	−0.31*	0.40	0.01	<0.001
Osmunda regalis	Or	−0.42*	0.24	−0.27	0.09	−0.31*	0.31
Pinus elliottii	Pe	−0.17*	0.36	−0.23*	0.55	0.13	0.15
Pinus taeda	Pt	−0.55*	0.54	−0.42*	0.56	−0.25	0.25
Quercus laurifolia	Ql	−0.18*	0.21	−0.09	0.13	−0.14	0.07
Quercus nigra	Qn	−0.37*	0.61	−0.28*	0.44	−0.21	0.18
Taxodium distichum	Td	−0.33*	0.58	−0.35*	0.52	0.06	0.06

*Statistical significance for the regression as well as the change, with $P < 0.05$.

with a relative sensitivity of only −17% and −18% per 100 ppm, whereas *P. taeda* shows the strongest sensitivity in g_{smax}, with −55% per 100 ppm. Despite these differences in response rate, the total change exceeds the maximum intrinsic variability quantified as the root mean square error (RMSE) in all species (Table S2). The CO_2-induced phenotypic decrease in g_{smax} on decadal timescales resembles evolutionary g_{smax} adaptation over geological timescales (32), reflecting the permanent attempt of plants to optimize individual fitness.

As on geological timescales (8), combined values of D and a_{max} on which the calculation of g_{smax} is based here are negatively correlated and follow a power law relationship in which high values of D are accompanied by low a_{max} values, and vice versa (Fig. 3). For individual species, however, D and a_{max} are confined to specific ranges forming clusters distributed along this power law, where significant negative correlations are also apparent in five out of nine individual clusters (*P. elliottii*, *T. distichum*,

Fig. 3. The measured stomatal density [D (mm^{-2})] and pore size [a_{max} (μm^2)] of nine common species in Florida ($n = 667$) (species names and abbreviations as in Table 1). The clusters depict a phenotypical range of D and a_{max} for each species under changing conditions of the past 150 y. Approximate lower limits are $D = \approx 20$ mm^{-2} and $a_{max} = \approx 15$ μm^2. Multiple combination of D and a_{max} can lead to the same g_{smax} value (mol·m^{-2}·s^{-1}), indicated by the black curved lines.
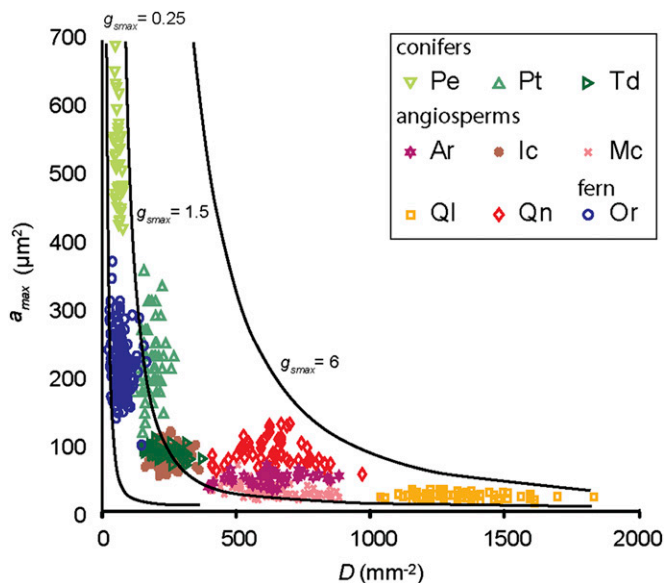
Q. laurifolia, *M. cerifera*, and *O. regalis*; Table S3). This implies that the clusters represent the phenotypic plasticity of the various species, showing adjustments of both D and a_{max} that occurred in response to the complex of environmental perturbations to which the sampled vegetation was exposed, including CO_2.

Within the total dataset, the most prominent difference exists between the angiosperm clusters with many small stomata that display large diversity in D and the conifers and fern clusters with few large stomata that display large diversity in a_{max}. The position of individual species on this power law curve likely represents their different evolutionary history (33, 34), with an earlier design for conifers and ferns and a more innovative design for angiosperms. Nevertheless, different combinations of D and a_{max} can lead to the same g_{smax} (Fig. 3) and the same decrease in g_{smax} in response to rising CO_2 (Table 1).

Testing the CO_2 sensitivity of D and a_{max} individually, we observe that the plastic response of D is always negative and more pronounced than in a_{max} (Table 1). This consistent decrease of D under rising CO_2 has already been reported for the angiosperm and fern species in our dataset (26, 27). We now complement the range of species known to reduce D in response to rising CO_2 by including the conifers *P. elliottii*, *P. taeda*, and *T. distichum*. Over the sampled CO_2 rise in CO_2, the relative sensitivity in D varies from maximal −42% per 100 ppm in *P. taeda* to minimal −9% per 100 ppm in *Q. laurifolia* (Table 1) ($P < 0.05$ for all but *O. regalis* and *Q. laurifolia*, with $P = 0.12$ and $P = 0.10$, respectively). The total change in D exceeds the maximum intrinsic variability quantified as the RMSE in all species except *O. regalis* and *Q. laurifolia* (Table S4). These rates are broadly consistent with decreases in D reported for European tree species grown under anthropogenic CO_2 increase (12, 13, 15, 35).

Focusing on the changes in a_{max} over the sampled CO_2 increase, weak and unidirectional relations are observed. Significant relations were only found for *A. rubrum* and *O. regalis*, which show reductions in a_{max} of −27% and −31% per 100 ppm, respectively (Table 1). Moreover, the changes in our a_{max} data series only exceed the RMSE for five of the species studied (Table S5). This variable response is different from changes in a_{max} to anthropogenic CO_2 rise reported earlier for two European tree species, for which a weak increase was observed (13, 36). From these observations it is apparent that D is highly sensitive to rising CO_2, whereas changes in a_{max} are variable between species and seem to be governed independently.

Because it is hypothesized that the different leaf structures, in particular leaf vein density, of angiosperms and conifers (31) result in different epidermal structural responses to rising CO_2, we compared the general relative sensitivities of the two plant groups in our dataset. Results show that coniferous species seem
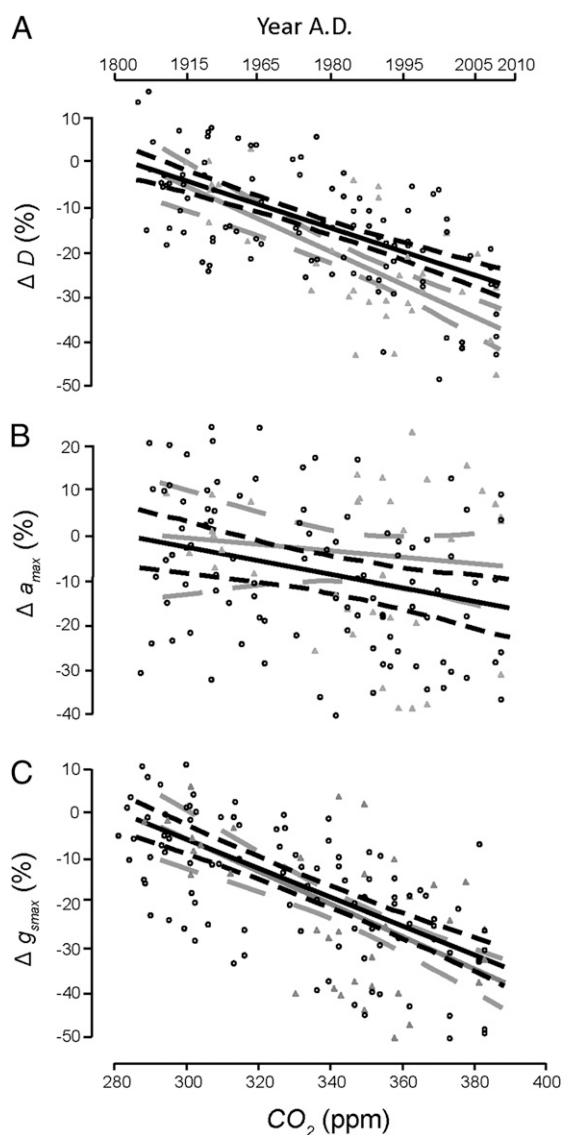
to respond with a significantly stronger decrease in D (slope, -35% per 100 ppm) than angiosperms (slope, -27% per 100 ppm) (Fig. 4A and Table S6). Conversely, angiosperms respond with an apparent but not significantly stronger decrease in a_{max} (slope, -15% per 100 ppm) compared with the conifers (slope, -7% per 100 ppm). Conifers also display a much larger range of variability, indicated by the broader confidence interval (Fig. 4B). Despite these differences, a highly comparable overall decrease in g_{smax} to a rise of CO_2 from preindustrial to present in angiosperms (slope, -33% per 100 ppm) and conifers (slope, -37% per 100 ppm) emerges from this combination (Fig. 4C). Summarizing, our data show that both angiosperms and conifers exhibit a similar response in g_{smax} to the anthropogenic rise in CO_2.

Fig. 4. Relative sensitivity in D (A), a_{max} (B), and g_{smax} (C) of the grouped angiosperm species (black line, black dots) and coniferous species (gray line, gray triangles) over the sampled CO_2 increase since the industrial revolution. Dashed lines depict 95% confidence intervals for angiosperms (black short dashed lines) and conifers (gray long dashed lines). (SE, r^2, and P values given in Table S6). Only D is significantly different between angiosperms and conifers ($P < 0.001$).

Discussion

The presented data reveal that the nine species from Florida reduce their g_{smax} in response to the industrial CO_2 rise via D and a_{max} adaptation within their phenotypic plasticity. This likely represents the plants' adaptation to increase $iWUE$ by optimizing carbon gain to water loss (11, 37). We demonstrate that adaptation of g_{smax} is achieved by species-specific strategies to alter D and/or a_{max}. The overall decrease in g_{smax} is predominantly the result of a general and significant reduction of D in response to rising CO_2 in all species, whereas a_{max} seems to adapt to other environmental conditions as well, because no consistent relation with CO_2 was observed. However, the importance of including D as well as a_{max} in the reconstruction of g_{smax} is emphasized by the generally improved correlation of g_{smax} with CO_2, compared with D and a_{max} separately (Table 1). The observed change in a_{max} opposes the positive relation between pore size and CO_2 found over geological timescales (8). This discrepancy can be explained by considering that on the timescale studied here plants adapt within their phenotype and not genotype to reduce g_{smax}, which is most efficiently done by reducing rather than increasing pore size. This suggests that plants can and do adapt to changing conditions by fine-tuning D and a_{max} plastically to optimize their individual fitness.

Despite the consistent trend observed in g_{smax}, considerable variability characterizes the individual D and a_{max} data series, and consequently g_{smax}, because climatic and site-specific environmental factors such as light, temperature, and water availability affect D and a_{max} as well (22, 24, 25). Even though the long-term mean temperature and precipitation in Florida have not changed over the past 150 y, strong interannual temperature and precipitation fluctuations (Fig. 1) caused by the El Niño/Southern Oscillation (ENSO) and Atlantic Multidecadal Oscillation teleconnections (38, 39) may in part have caused D and a_{max} variability. Indeed, short-term changes in epidermis morphology in *Q. laurifolia* have been linked to ENSO-tied winter precipitation (25). Together with D and a_{max} diversity throughout the canopy and even within the same leaf (40), these environmental factors produce substantial scatter in the data. Consequently, sampling on low temporal resolution might explain the lack of evidence for CO_2-induced $iWUE$ adaptation as in herbarium studies covering 2 to 5 selected years only (41). The present study therefore emphasizes the necessity of sufficiently high-resolution as well as multidecadal data series to elucidate the long-term subtle response of g_{smax} to changing CO_2.

The large variation in reconstructed g_{smax} values reflect the difference in leaf vascular architecture, whereby the high vein density typical for angiosperms allows for high g_{smax} and the low vein density in ferns and conifers is reflected by low g_{smax} (31, 42). The differences in the leaf hydraulic systems between angiosperms and conifers are also expressed in their position on the power law relation between D and a_{max}. Angiosperms reach high g_{smax} with numerous small stomata, and conifers reach lower g_{smax} with fewer large stomata (8). These findings can be placed against an evolutionary background, where ferns and conifers evolved in a higher-than-present CO_2 world, in which lower g_{smax} would be perfectly sufficient to maintain high photosynthesis. The late Cretaceous drop in CO_2 likely triggered the expansion of the leaf-vascular network in angiosperms (9), allowing them to attain higher photosynthesis rates than conifers and ferns but at the cost of high carbon and transpirational water loss (3). This water loss in angiosperms might be minimized as small stomata are faster to close than large stomata under desiccating conditions (43). Moreover, a consequence of the associated high water loss is the resulting evaporative cooling, which maintains an optimal leaf temperature (44). Our data thus show that species-specific g_{smax} is determined in part by evolutionary adaptation to conditions in which they evolved.

When exposed to decadal variability the species studied adapt within the limits of their phenotypic plasticity, by adjusting D and a_{max}. Despite the large differences in D and a_{max} between species, even within the same genus they all exhibit highly comparable adaptation of g_{smax} to increasing CO_2. Comparing the general adaptation of the angiosperms and conifers as groups, however, a different strategy to reduce g_{smax} was observed, depending on their position on the power law curve. Although only the relative change in D between angiosperms and conifers is significantly different, the tendency towards an opposite response in D and a_{max} does illustrate that variable adaptations lead to the same reduction in g_{smax}. These results can be explained by the different position on the power law curve, whereby species reduce g_{smax} most efficiently by changing either D or a_{max} to get the steepest gradient in g_{smax} (Fig. 2). Because the construction of an extended vascular network is coupled to high carbon costs (3, 42), it was hypothesized before that angiosperms reduce g_{smax} more than conifers and ferns. However, our data show a highly comparable sensitivity to the industrial CO_2 rise in all groups sampled and thereby demonstrate the underlying principle that plants generally optimize their leaf structure in response to rising CO_2, apparently irrespective of their leaf architecture.

Having discussed the responses and possible underlying mechanisms, the potential further development of g_{smax} under future increasing CO_2 can be evaluated. The $iWUE$ responses measured in short-term growth experiments over below-present to present CO_2 levels are also found to be comparable in angiosperms, conifers, and ferns, but the trends diverge from present to elevated CO_2, where the response in conifers and ferns levels off (45). Our results of structural adaptation from ≈280 ppm to 387 ppm CO_2 does not bear any evidence for a diverging response between plant lineages. Whether any g_{smax} off-leveling will occur under continuing CO_2 enrichment, and at what CO_2 concentration this will happen, should be estimated by modeling exercises incorporating adaptation within the species-specific phenotypic plasticity (37).

In conclusion, our results point to a common mechanism in C3 plants to reduce maximum stomatal conductance via adjustment of stomatal density and pore size within the limits of their phenotypic plasticity on a decadal timescale. As atmospheric carbon dioxide concentration is rising, plants can and do reduce water loss by reducing maximal stomatal conductance while maintaining carbon uptake (3, 31). Further decreases in stomatal conductance have been observed at CO_2 rising above present levels in FACE short-term experiments (21) and in fossil leaves over geological timescales (8). Both lines of evidence, however, fall beyond or below the timescales of the projected rate of continuing CO_2 increase, which is likely to surpass the time needed for adaptation via natural selection. Consequently, the adaptation within the phenotypic plasticity is likely to constrain epidermis structural adaptation in the near future when pheno-typic response limits are reached (35, 37). Current increase in CO_2 and the coinciding reduction in plant transpiration already results in increased continental run-off (46), and climate models predict surface temperature increases arising from reduced evaporative cooling (6, 7). The mechanisms of optimization of carbon gain to water loss described here could be used to better estimate this physiological forcing for the past and future CO_2 but should be considered within the framework of species-specific phenotypic plasticity (37).

Materials and Methods

Sample Preparation and Analysis. The leaf fragments were treated in 4% sodium hypochlorite ($NaClO_2$) at 40 °C for several minutes up to 24 h, after which the stomata-bearing abaxial cuticle could be peeled off from the mesophyll, dyed with saffranine, and mounted in glycerine jelly. Because *Pinus* has an approximately equal amount of stomata on the abaxial as well as the adaxial surface, the entire cuticle was processed. Standardized, computer-aided analysis of the epidermal properties was performed on Leica Quantimet 500C/500+ and AnalySIS image analysis systems. Stomatal density (D; number of stomata·m^{-2}) was measured on 5–10 alveoles of each leaf sample and averaged. Because of different epidermis cell patterning, *Pinus* is measured with the stomatal rows running diagonally in the image. Pore length (L; μm) is determined by averaging measurements of ≈25 stomata for each sample. Data are available upon request.

Calculating g_{smax} to Water Vapor. To determine the stomatal conductance to water vapor g_{smax} (mol·m^{-2}·s^{-1}), the equation provided by Franks and Farquhar (17) is applied, using a two-way end correction accounting for the diffusion shells (8) (Eq. 1). Maximum pore surface area a_{max} (m^2) is defined as an ellipse and quantified as $\pi \cdot L^2/8$, with L being stomatal pore length (m). Stomatal pore depth l (m) is assumed to be equal to the guard cell width of the stomata when the guard cell is fully inflated (8). Quantification of l follows from the significant positive linear relations between pore length and guard cell width for each species, with exception of *P. taeda*, for which a constant value is taken (Table S7). Values used for gas constants d and v are those for 25 °C. For the determination of the long-term relative sensitivities of the measured D and a_{max}, and consequent g_{smax}, the regressions are performed on values averaged per sampled year.

Statistical Analyses. The significance of the observed regressions presented here is tested in three steps, with P values of <0.05 considered statistically significant. First, the significance of each regression plotted through the data series was tested. Second, using a Student t test on the slopes of these regressions, it was determined whether the observed changes were significantly larger than 0. Finally, to test whether the average responses in D, a_{max}, and g_{smax} were significantly different between angiosperms and conifers, a t test (two samples assuming unequal variances) was performed on the pooled data of each group within the CO_2 interval of 360–387 ppm.

1. Cowan IR, Farquhar GD (1977) Stomatal function in relation to leaf metabolism and environment. *Integration of Activity in the Higher Plants*, ed Jennings DH (Cambridge Univ Press, Cambridge, UK), pp 471–505.
2. Raven JA (2002) Selection pressures on stomatal evolution. *New Phytol* 153:371–386.
3. Beerling DJ, Franks PJ (2010) Plant science: The hidden cost of transpiration. *Nature* 464:495–496.
4. Bonan GB (2008) Forests and climate change: Forcings, feedbacks, and the climate benefits of forests. *Science* 320:1444–1449.
5. Betts RA, et al. (2007) Projected increase in continental runoff due to plant responses to increasing carbon dioxide. *Nature* 448:1037–1041.
6. Andrews T, Doutriaux-Boucher M, Boucher O, Forster PM (2010) A regional and global analysis of carbon dioxide physiological forcing and its impact on climate. *Clim Dyn*, 10.1007/s00382-010-0742-1.
7. Cao L, Bala G, Caldeira K, Nemani R, Ban-Weiss G (2010) Importance of carbon dioxide physiological forcing to future climate change. *Proc Natl Acad Sci USA* 107:9513–9518.
8. Franks PJ, Beerling DJ (2009) Maximum leaf conductance driven by CO_2 effects on stomatal size and density over geologic time. *Proc Natl Acad Sci USA* 106:10343–10347.
9. Brodribb TJ, Feild TS (2010) Leaf hydraulic evolution led a surge in leaf photosynthetic capacity during early angiosperm diversification. *Ecol Lett* 13:175–183.
10. Farquhar GD, Dubbe DR, Raschke K (1978) Gain of the feedback loop involving carbon dioxide and stomata: Theory and measurement. *Plant Physiol* 62:406–412.
11. Katul G, Manzoni S, Palmroth S, Oren R (2010) A stomatal optimization theory to describe the effects of atmospheric CO_2 on leaf photosynthesis and transpiration. *Ann Bot (Lond)* 105:431–442.
12. Woodward FI (1987) Stomatal numbers are sensitive to increases in CO_2 from pre-industrial levels. *Nature* 327:617–618.
13. Wagner F, et al. (1996) A natural experiment on plant acclimation: Lifetime stomatal frequency response of an individual tree to annual atmospheric CO_2 increase. *Proc Natl Acad Sci USA* 93:11705–11708.
14. Kürschner WM, van der Burgh J, Visscher H, Dilcher DL (1996) Oak leaves as biosensors of late neogene and early pleistocenepaleoatmospheric CO_2 concentrations. *Mar Micropaleontol* 27:299–312.
15. Wagner F, Kouwenberg LLR, van Hoof TB, Visscher H (2004) Reproducibility of Holocene atmospheric CO_2 records based on stomatal frequency. *Quat Sci Rev* 23:1947–1954.

Lammertsma et al.

ENVIRONMENTAL SCIENCES

16. Lake JA, Woodward FI, Quick WP (2002) Long-distance CO_2 signalling in plants. *J Exp Bot* 53:183–193.

17. Franks PJ, Farquhar GD (2001) The effect of exogenous abscisic acid on stomatal development, stomatal mechanics, and leaf gas exchange in *Tradescantia virginiana*. *Plant Physiol* 125:935–942.

18. Farquhar GD, Sharkey TD (1982) Stomatal conductance and photosynthesis. *Annu Rev Plant Physiol* 33:317–345.

19. Long SP, Ainsworth EA, Rogers A, Ort DR (2004) Rising atmospheric carbon dioxide: Plants FACE the future. *Annu Rev Plant Biol* 55:591–628.

20. Reid CD, et al. (2003) On the relationship between stomatal characters and atmospheric CO_2. *Geophys Res Lett* 30:1983–1986.

21. Ainsworth EA, Rogers A (2007) The response of photosynthesis and stomatal conductance to rising [CO_2]: Mechanisms and environmental interactions. *Plant Cell Environ* 30:258–270.

22. Royer DL (2001) Stomatal density and stomatal index as indicators of paleoatmospheric CO_2 concentration. *Rev Palaeobot Palynol* 114:1–28.

23. Poole I, Kürschner WM (1999) Stomatal density and index: The practice. *Fossil Plant and Spores: Modern Techniques*, eds Jones TP, Rowe NP (Geological Society, London), pp 257–260.

24. Franks PJ, Drake PL, Beerling DJ (2009) Plasticity in maximum stomatal conductance constrained by negative correlation between stomatal size and density: An analysis using *Eucalyptus globulus*. *Plant Cell Environ* 32:1737–1748.

25. Wagner-Cremer F, Donders TH, Visscher H (2010) Drought stress signals in modern and subfossil *Quercuslaurifolia* (Fagaceae) leaves reflect winter precipitation in southern Florida tied to El Niño-Southern Oscillation activity. *Am J Bot* 97:753–759.

26. Neftel A, et al. (1994) Trends: A compendium of data on global change. Available at: http://cdiac.ornl.gov/trends/co2/contents.htm. Accessed February, 2010.

27. Keeling CD, Whorf TP (2003) Atmospheric CO_2 concentrations—Mauna Loa Observatory, Hawaii, 1958–2003. Available at: http://cdiac.ornl.gov/pns/pns_main.html. Accessed February, 2010.

28. Wagner F, Dilcher DL, Visscher H (2005) Stomatal frequency responses in hardwood-swamp vegetation from Florida during a 60-year continuous CO_2 increase. *Am J Bot* 92:690–695.

29. Wagner F, Visscher H, Kürschner WM, Dilcher DL (2007) Influence of ontogeny and atmospheric CO_2 on stomata parameters of *Osmundaregalis*. *Cour Forsch Inst Senckenberg* 258:183–189.

30. Donders TH, Wagner F, Van der Borg K, De Jong AFM, Visscher H (2004) A novel approach for developing high-resolution sub-fossil peat chronologies with ^{14}C dating. *Radiocarbon* 46:455–464.

31. Brodribb TJ, Holbrook NM, Zwieniecki MA, Palma B (2005) Leaf hydraulic capacity in ferns, conifers and angiosperms: Impacts on photosynthetic maxima. *New Phytol* 165:839–846.

32. Franks PJ, Beerling DJ (2009) CO_2-forced evolution of plant gas exchange capacity and water-use efficiency over the Phanerozoic. *Geobiology* 7:227–236.

33. Dilcher D (2000) Toward a new synthesis: Major evolutionary trends in the angiosperm fossil record. *Proc Natl Acad Sci USA* 97:7030–7036.

34. Henry RJ (2005) *Plant Diversity and Evolution: Genotypic and Phenotypic Variation in Higher Plants* (Centre for Agricultural Bioscience International, Wallingford, UK), p 332.

35. Kürschner WM (1997) The anatomical diversity of recent and fossil leaves of the durmast oak (*Quercuspetraea*Lieblein/*Q. pseudocastanea*Goeppert)—implications for their use as biosensors of palaeoatmospheric CO_2 levels. *Rev Palaeobot Palynol* 96:1–30.

36. Garcia-Amorena I, Wagner F, van Hoof TB, Gómez Manzaneque F (2006) Stomatal responses in deciduous oaks from southern Europe to the anthropogenic atmospheric CO_2 increase; refining the stomatal-based CO_2 proxy. *Rev Palaeobot Palynol* 141:303–312.

37. De Boer HJ, et al. (2011) Climate forcing due to optimization of maximal leaf conductance in subtropical vegetation under rising CO2. *Proc Natl Acad Sci USA*, 10.1073/pnas.1100555108.

38. Donders TH, Wagner F, Dilcher DL, Visscher H (2005) Mid- to late-Holocene El Nino-Southern Oscillation dynamics reflected in the subtropical terrestrial realm. *Proc Natl Acad Sci USA* 102:10904–10908.

39. Curtis S (2008) The Atlantic Multidecadal Oscillation and extreme daily precipitation over the US and Mexico during the hurricane season. *Clim Dyn* 30:343–351.

40. Poole I, Weyers JDB, Lawson T, Raven JA (1996) Variations in stomatal density and index: Implications for palaeoclimatic reconstructions. *Plant Cell Environ* 19:705–712.

41. Miller-Rushing AJ, Primack RB, Templer PH, Rathbone S, Mukunda S (2009) Long-term relationships among atmospheric CO_2, stomata, and intrinsic water use efficiency in individual trees. *Am J Bot* 96:1779–1786.

42. McKown AD, Cochard H, Sack L (2010) Decoding leaf hydraulics with a spatially explicit model: Principles of venation architecture and implications for its evolution. *Am Nat* 175:447–460.

43. Hetherington AM, Woodward FI (2003) The role of stomata in sensing and driving environmental change. *Nature* 424:901–908.

44. Upchurch DR, Mahan JR (1988) Maintenance of constant leaf temperature by plants—II. experimental observations in cotton. *Environ Exp Bot* 28:359–366.

45. Brodribb TJ, McAdam SAM, Jordan GJ, Feild TS (2009) Evolution of stomatal responsiveness to CO_2 and optimization of water-use efficiency among land plants. *New Phytol* 183:839–847.

46. Gedney N, et al. (2006) Detection of a direct carbon dioxide effect in continental river runoff records. *Nature* 439:835–838.